Separating the effects of albedo from eco-physiological changes on surface temperature along a successional chronosequence in the southeastern United States

Jehn-Yih Juang,[1,2] Gabriel Katul,[1,3] Mario Siqueira,[1,4] Paul Stoy,[1,5] and Kimberly Novick[1]

Received 24 July 2007; revised 2 October 2007; accepted 15 October 2007; published 15 November 2007.

[1] In the southeastern United States (SE), the conversion of abandoned agricultural land to forests is the dominant feature of land-cover change. However, few attempts have been made to quantify the impact of such conversion on surface temperature. Here, this issue is explored experimentally and analytically in three adjacent ecosystems (a grass-covered old-field, OF, a planted pine forest, PP, and a hardwood forest, HW) representing a successional chronosequence in the SE. The results showed that changes in albedo alone can warm the surface by 0.9°C for the OF-to-PP conversion, and 0.7°C for the OF-to-HW conversion on annual time scales. However, changes in eco-physiological and aerodynamic attributes alone can cool the surface by 2.9 and 2.1°C, respectively. Both model and measurements consistently suggest a stronger over-all surface cooling for the OF-to-PP conversion, and the reason is attributed to leaf area variations and its impacts on boundary layer conductance. **Citation:** Juang, J.-Y., G. Katul, M. Siqueira, P. Stoy, and K. Novick (2007), Separating the effects of albedo from eco-physiological changes on surface temperature along a successional chronosequence in the southeastern United States, *Geophys. Res. Lett.*, *34*, L21408, doi:10.1029/2007GL031296.

1. Introduction

[2] Radiative perturbations due to land-cover changes are considered among the strongest climate forcing mechanisms at global and regional scales [e.g., *Cess*, 1978; *Charney et al.*, 1977; *Otterman*, 1977]. Small changes in surface albedo (α_s), even below detection limits of existing satellite-derived products, can lead to global temperature changes equivalent to that attributable to the anthropogenic increase of any enhanced greenhouse gas [*Charlson et al.*, 2005]. Regional modeling studies have documented that the positive forcing induced by decreased α_s in boreal forests can be sufficiently large to offset the negative forcing expected from increased carbon sequestration by these forests [*Betts*, 2000]. Other studies also found that historical land-cover conversion in mid-latitude agricultural regions may have decreased air temperature (T_a) by 1–2°C, primarily due to the role of α_s [*Feddema et al.*, 2005].

[3] In the SE, the conversion of abandoned agricultural land to forested ecosystems via both ecological succession and plantation forestry has been a dominant feature of land use change since post-Civil War reconstruction and the 1950s, respectively. Few attempts have been made to quantify the impact of land cover change on T_a in the SE. Over the next 40 years, the area of land populated by pine plantations within the SE is projected to increase from 0.13 to 0.22 million km^2, with concomitant declines in upland hardwood forested area from 0.27 to 0.23 million km^2, and agricultural land from 0.40 to 0.26 million km^2 [*Wear and Greis*, 2002]. Given the large annual incident shortwave radiation in the SE, albedo changes ($\delta\alpha_s$) due to such ecosystem conversion may result – and may have already resulted - in significant changes in air temperature (δT_a), (hereafter δ refers to the land-use conversion induced perturbation). However, albedo alterations are not the only effect of land use change; bulk canopy conductance (g_b) and surface emissivity (ε_s) also change upon ecosystem conversion. Thus, the relative importance of all land surface changes (radiative, aerodynamic, or physiological) must be jointly explored.

[4] In an era of rapid land-cover changes, maximum δT_a occurs when all changes in surface temperature (δT_s) translate to air temperature (i.e., maximum (δT_a) $\approx \delta T_s$) at regional scales. Hence, by exploring the influence of land conversion on δT_s through $\delta\alpha_s$, $\delta\varepsilon_s$, and δg_b, locally (i.e. at the field scale) we can constrain the upper limits in expected δT_a due to these factors.

[5] As a necessary first step towards progressing on this objective, δT_s was measured and modeled from $\delta\alpha_s$, $\delta\varepsilon_s$, and δg_b using data collected from three adjacent ecosystems representing the two end-members and an intermediate stage of a successional gradient in the SE, shown in Figure 1 [*Johnston and Odum*, 1956]. The ecosystems, all experiencing similar climatic and edaphic conditions, include an abandoned agricultural grass-covered old-field (OF), a planted pine forest (PP), and a hardwood forest (HW). Here, we report on $\delta\alpha_s$, $\delta\varepsilon_s$, and δg_b estimated from heat flux and radiation measurements across these three sites, and explore the relative importance of albedo with respect to the remaining factors on observed annual δT_s.

2. Study Site

[6] The three ecosystems are located within the Blackwood Division of Duke Forest near Durham, NC (35°58′N, 79°05′W, 163 m above sea level, see Figure 1) and are part

[1]Nicholas School of the Environment and Earth Sciences, Duke University, Durham, North Carolina, USA.
[2]Now at Department of Geography, National Taiwan University, Taipei, Taiwan.
[3]Department of Civil and Environmental Engineering, Duke University, Durham, North Carolina, USA.
[4]Departamento de Engenharia Mecânica, Universidade de Brasília, Brazil.
[5]Now at School of GeoSciences, University of Edinburgh, Edinburgh, UK.

0094-8276/07/2007GL031296

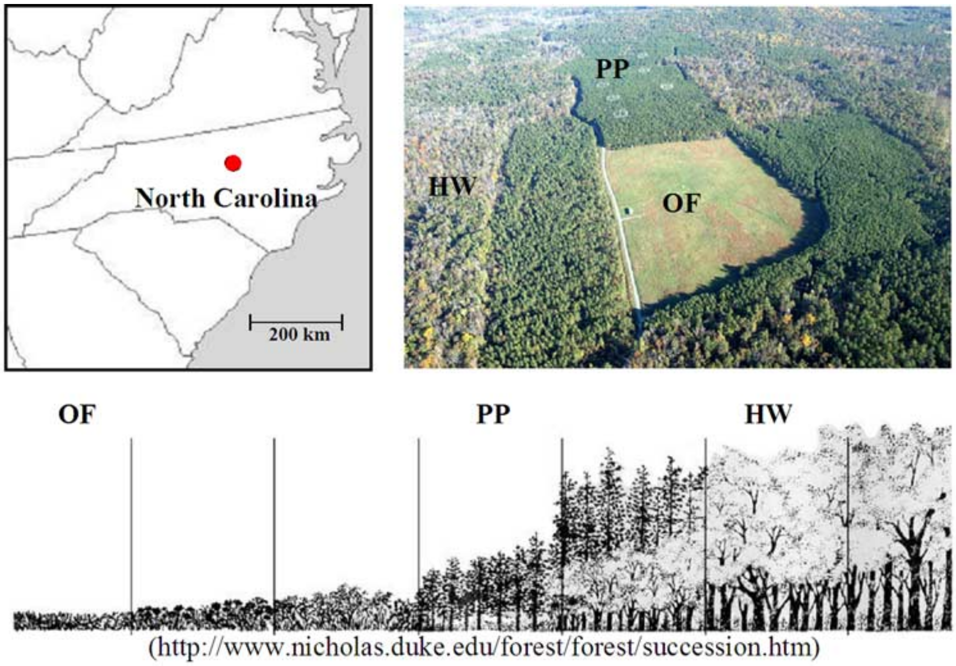

Figure 1. (top) (left) The location of the three AmeriFlux sites at the Blackwood Division of the Duke Forest, near Durham, North Carolina. (right) An aerial photograph of the three sites in autumn showing the brighter land-cover at OF relative to HW and PP. As a scale, the distance between the left (west) and right (east) edges of OF is about 305 m. (bottom) A typical succession in the SE after agricultural fields are abandoned (courtesy the Duke Forest Web site after *Johnston and Odum* [1956]).

of FLUXNET, an on-going global long-term micrometeorological monitoring initiative [*Baldocchi et al.*, 2001]. The mean annual precipitation (since 1948) is 1185 ± 177 mm, and the annual mean air temperature is 14.9 ± 0.9°C. The local topographic variations in the vicinity are small enough (slope < 5%), such that the effects of complex terrain on the flow statistics is negligible [*Siqueira et al.*, 2002].

[7] In each ecosystem, a meteorological tower was available to sample long-term environmental data and near surface eddy-covariance (EC) fluxes. The turbulent sensible heat (H) and latent heat (LE) fluxes were measured above the canopy using an EC system comprised of a LI-7500 open-path CO_2/H_2O gas analyzer (Li-Cor Inc., Lincoln, Nebraska) and a CSAT3 tri-axial sonic anemometer (Campbell Scientific Inc., Logan, Utah). The net radiation (R_n) and both long-wave and short-wave (incoming and outgoing) radiation were sampled using Kipp & Zonen CNR-1 net radiometers (Kipp & Zonen USA Inc., Bohemia, New York) since 2004. Details about each site, the experimental setup (for OF, see *Novick et al.* [2004]; for HW and PP, see *Oren et al.* [1998], *Stoy et al.* [2005], and *Pataki and Oren* [2003]), and the data processing are described elsewhere [*Katul et al.*, 1997; *Stoy et al.*, 2005]. The analysis here covers a two-year period (2004–2005), during which soil moisture did not limit transpiration apart from an acute drought in the latter part of the 2005 growing season [*Stoy et al.*, 2006a].

3. Theory

[8] The energy balance at the land-surface are given by

$$R_n = (1 - \alpha_s)R_{si} - \varepsilon_s \sigma T_s^4 + R_{li} = LE + H + G_s, \qquad (1)$$

where R_{si} and R_{li} are incident shortwave and downward longwave radiations, respectively (W m^{-2}); σ is the Stefan-Boltzmann constant (= 5.67×10^{-8} J K^{-4} m^{-2} s^{-1}), and G_s are the combined soil and storage heat fluxes. α_s is defined as the ratio of outgoing to incident short-wave radiation. Because these ecosystems are within 1 km of each other (Figure 1), they experience almost identical R_{si} and R_{li} on both hourly and annual time scales. From the CNR-1 radiation measurements available at the three sites, a regression analysis confirmed that both R_{si} and R_{li} were indistinguishable over the two year study period (for R_{si}, the regressions are $R_{si,\mathrm{PP}} = 0.99\mathrm{R}_{si,\mathrm{OF}} - 2.53$, $R^2 = 1.00$, and $R_{si,\mathrm{HW}} = 0.99\mathrm{R}_{si,\mathrm{OF}} - 1.61$, $R^2 = 0.99$; for R_{li}, the regression are $R_{li,\mathrm{PP}} = 1.02R_{li,\mathrm{OF}} - 11.76$, $R^2 = 0.99$, and $R_{li,\mathrm{HW}} = 0.99R_{li,\mathrm{OF}} - 7.98$, $R^2 = 0.99$, well within the expected accuracy of the CNR-1 radiometer; all regression statistics were based on half-hourly averaging intervals).

[9] Since this region is sufficiently humid, the latent heat flux (i.e. including evaporation and transpiration) may be modeled from a Priestley-Taylor like equation [*Priestley and Taylor*, 1972]:

$$LE = \alpha_{PT} \frac{\Delta}{\Delta + \gamma}(Q_n), \qquad (2)$$

where $Q_n = R_n - G_s$, Δ is the slope of the saturation vapor pressure- temperature curve, γ is the psychrometric constant (i.e. the ratio of specific heat of moist air at constant pressure C_p to the latent heat of vaporization of water L_v), and α_{PT} is the Priestley-Taylor parameter. For short vegetation (or bare soil), $\alpha_{PT} \approx 1.25$ was determined for well-watered conditions [*Parlange and Katul*, 1992; *Stull*, 1988]. For tall-forested ecosystems, $\alpha_{PT} < 1$ due to the

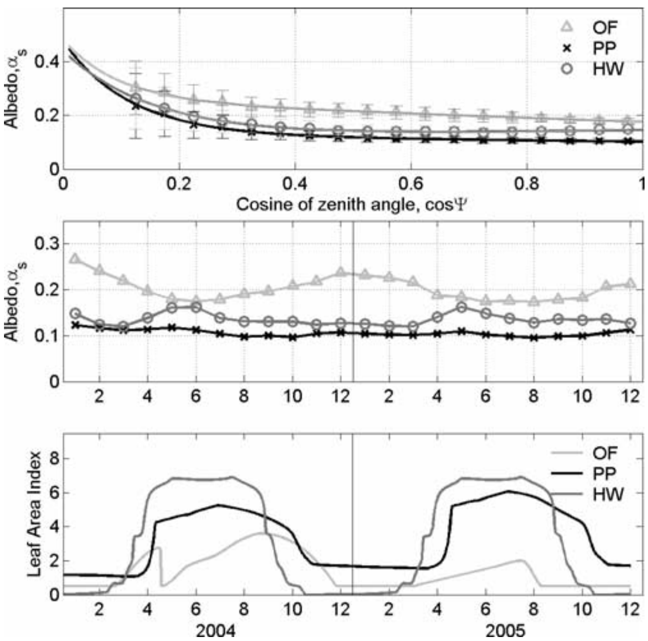

Figure 2. (top) The relationship between ensemble-averaged albedo and cosine of the zenith angle for the three ecosystems. Vertical bars are one standard deviation around the ensemble averages. (middle) Mid-day (1100 LT to 1400 LT) monthly ensemble-averaged albedo from 2004 to 2005 in the three ecosystems. (bottom) The variation in measured LAI (m^2 m^{-2}) in the three ecosystems. The large LAI excursions in OF are due to annual mowing for hay and to check woody encroachment.

added hydraulic resistance along the pathway from the soil to the atmosphere, even for wet soil conditions. H can be expressed as

$$H = Q_n\left(1 - \alpha_{PT}\frac{\Delta}{\Delta + \gamma}\right) = \rho C_p g_a (T_s - T_a), \qquad (3)$$

where ρ is the mean air density, and g_a is the bulk aerodynamic conductance. Let

$$\eta = \frac{\rho C_p g_a}{1 - \alpha_{PT}\frac{\Delta}{\Delta+\gamma}} = \frac{Q_n}{(T_s - T_a)},$$

so that T_s is given by the solution to the algebraic equation:

$$\varepsilon_s \sigma T_s^4 + \eta T_s = (1 - \alpha_s)R_{si} + R_{li} + \eta T_a - G_s. \qquad (4)$$

The left-hand side (LHS) of equation (4) is a function of T_s, η, and ε_s, while the right-hand side (RHS) is a function of α_s, η, and G_s. Our objective is to examine how land-use conversion, quantified by changes in α_s, η, and G_s, impacts T_s. Defining

$$\begin{aligned}\mathrm{LHS} &= f_1(\eta, T_s, \varepsilon_s) = \varepsilon_s \sigma T_s^4 + \eta T_s \\ \mathrm{RHS} &= f_2(\eta, \alpha_s, G_s) = (1 - \alpha_s)R_{si} + R_{li} + \eta T_a - G_s\end{aligned}$$

and considering only the first-order terms in the total derivative expansions results in

$$\begin{aligned} df_1 &= \left(\frac{\partial f_1}{\partial T_s}\delta T_s + \frac{\partial f_1}{\partial \eta}\delta\eta + \frac{\partial f_1}{\partial \varepsilon_s}\delta\varepsilon_s\right) = df_2 \\ &= \left(\frac{\partial f_2}{\partial \eta}\delta\eta + \frac{\partial f_2}{\partial \alpha_s}\delta\alpha_s + \frac{\partial f_2}{\partial G_s}\delta G_s\right).\end{aligned}$$

Hence, land-use conversion yields a concomitant δT_s:

$$\delta T_s = \frac{\left(\frac{\partial f_2}{\partial \eta} - \frac{\partial f_1}{\partial \eta}\right)\delta\eta + \frac{\partial f_2}{\partial \alpha_s}\delta\alpha_s + \frac{\partial f_2}{\partial G_s}\delta G_s - \frac{\partial f_1}{\partial \varepsilon_s}\delta\varepsilon_s}{\frac{\partial f_1}{\partial T_s}}.$$

[10] Using the definitions of f_1 and f_2, the following expression for δT_s can now be derived:

$$\delta T_s = \frac{1}{4\sigma\varepsilon_s T_s^3 + \eta}\left[\underset{\mathrm{I}}{(T_a - T_s)\delta\eta} - \underset{\mathrm{II}}{R_{Si}\delta\alpha_s} - \underset{\mathrm{III}}{\delta G_s} - \underset{\mathrm{IV.}}{\sigma T_s^4 \delta\varepsilon_s}\right] \qquad (5)$$

[11] Equation (5) shows the four major factors affecting δT_s following land-use conversion: Term I, an eco-physiological and aerodynamic component (recall that η is a function of bulk aerodynamic conductance and the Priestly-Taylor parameter), term II, an albedo component, term III, a heat storage change (expected to be small on annual time scales), and finally term IV, a thermal emissivity component.

[12] The relative importance of each of these factors is explored for two land-cover conversion scenarios: from OF to PP, and from OF to HW. These two conversions mimic the past (i.e. successional) and projected (i.e. timberland compositions) land-use changes in the region. Conversion from HW to PP is an important, but more minor, contributor to total land use conversion in the SE; effects thereof can be considered by noting the difference between these two conversions.

4. Results and Discussion

[13] Figure 2 (top) presents the relationship between ensemble measured α_s and solar zenith angle (ψ) for all three ecosystems. As evidenced by Figure 2, α_s in OF is generally higher than in PP and HW and increases gradually as ψ increases. The forested ecosystems maintained a near constant α_s for small ψ (i.e. $\cos\psi > 0.5$). Figure 2 (middle) shows monthly ensemble averaged α_s at mid-day (11:00 to 14:00 LT) over the two-year period. As expected, OF appeared 'brighter' than the two forested ecosystems, consistent with the image in Figure 1, yet exhibited strong seasonal variation in α_s; α_s remained almost constant ($\sim$0.1) over the entire two-year period for PP as expected for an evergreen forest; α_s tracked the seasonality in leaf area index (LAI) at HW, shown in Figure 2 (bottom).

[14] The radiometer inferred T_s (hereafter referred to as measured) in each ecosystem was computed from the CNR-1 measured emitted long-wave radiation (R_{lo}) using $R_{lo} = \sigma\,\varepsilon_s\, T_s^4$, where ε_s can vary across different ecosystems and exhibit seasonal variations within a given ecosystem due to seasonal changes in surface characteristics. Because no

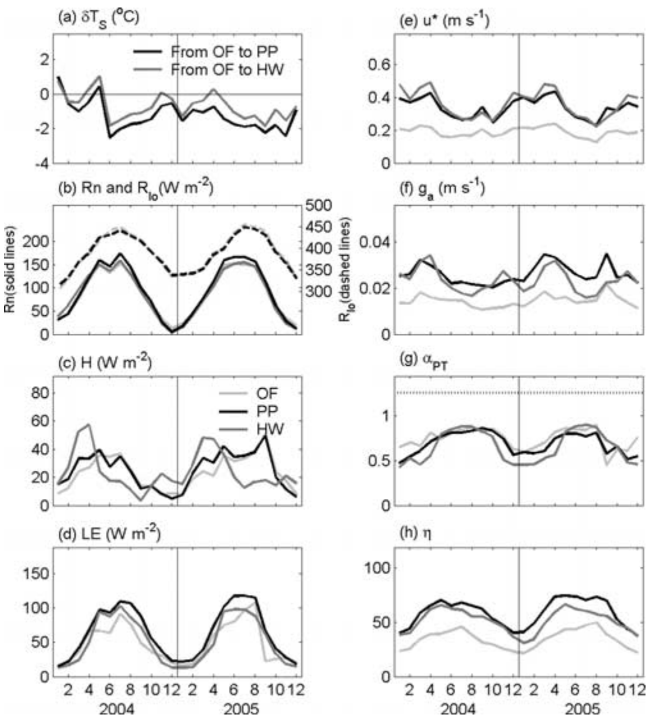

Figure 3. (a) Monthly averaged changes in surface temperature estimated from the longwave radiation measurements for both land-cover changes (OF to PP and OF to HW). (b) to (e) The variations (monthly average) of H, LE, R_n, R_{lo}, and friction velocity u*. (f) to (g) The variations (monthly average) of the calculated g_a, α_{PT}, and η in these ecosystems. The maximum value $\alpha_{PT} = 1.25$ in Figure 3g, shown as reference, is for well-watered conditions and short canopies.

precise measurements were locally available for ε_s, we derived an empirical relationship between literature reported α_s and ε_s [*Campbell and Norman*, 1998; *Chen and Sun-Mack*, 2002] for crops and forests in temperate regions, ($\varepsilon_s = -0.16\alpha_s + 0.99$, $R^2 = 0.94$), and used this derived expression to empirically model seasonal variations in ε_s from measured variations in α_s. ε_s then were used to compute T_s for each ecosystem from measured R_{lo}.

[15] Figure 3 shows the measured δT_s estimated from R_{lo} in all three ecosystems. The comparison suggests a cooling effect if OF is completely converted to PP or HW. Note that the cooling effect by converting OF to PP is roughly 39% higher than the cooling effect obtained by converting OF to HW (−1.2°C versus −0.9°C in annual averages). Because the differences in R_{lo} across the different ecosystems are not large (Figure 3), it suggests that some of the observed difference in measured δT_s is due to differences in ε_s.

[16] In equation (5), terms II through IV can be determined from the EC-based flux measurements, also shown in Figure 3. However, η in term I must be calculated separately from g_a and α_{PT}, which can be inferred from the components of the measured energy budget, i.e. equations (1) to (3) and EC fluxes. Figure 3 compares the monthly variations in measured R_n, H, and LE in all three ecosystems. The variation in H in HW exhibits strong seasonality due to the dramatic changes in LAI (Figure 2). Furthermore, in late summer of 2005, the ecosystems experienced an acute drought, causing higher H in PP and OF, but not in HW. These two factors explain the canonical differences in H between HW and PP and why g_a in PP appears larger than HW. The fact that g_a in PP is larger than HW may, at first glance, appear to be counter-intuitive to the momentum sink because HW is a taller and rougher canopy (see friction velocity comparisons in Figure 3). However, the seasonality in LAI and the acute drought at the end of 2005 explain why the overall g_a in PP remains higher at longer time scales considered here.

[17] As for the variation in α_{PT}, the data here suggests that it is on the order of 0.5 during the winter seasons but increased up to 0.9 to 1.0 during the summer months. The variations in η estimated from g_a and α_{PT} in different ecosystems also show that the values of η in PP and HW are relatively higher by 70% and 50%, respectively, than η in OF. This significant difference could possibly lead to dramatic fluctuations in the eco-physiological/aerodynamic component of equation (5).

[18] Once all the components in equation (5) are resolved, we can examine how land-cover changes, quantified by changes in η, α_s, G_s and ε_s, impact δT_s. Figure 4 shows the calculated seasonal variation in each of these four components for both land cover conversions. It is clear that both the ground heat flux component (term III) and the thermal emissivity component (term IV) remain smaller than the other two components in influencing δT_s, as expected. These two small components may be (conveniently) neglected on annual time scales, at least when compared to albedo effects. Hence, it is safe to say from Figure 4 that δT_s is primarily dominated by the interplay between the two larger yet competing effects: albedo (term II) and the eco-physiology/aerodynamics (term I).

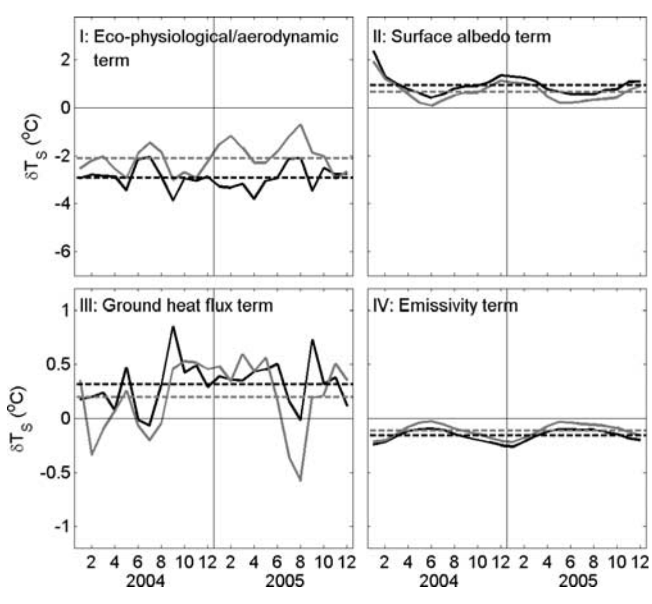

Figure 4. The contribution of each of the four components in equation (5) to δT_s. The black lines and dark gray lines refer to an OF to PP conversion and an OF to HW conversion, respectively, and the dashed lines represent long-term averages. Note the ordinate scale difference between Figure 4 (top) and 4 (bottom).

Table 1. Comparisons of the 2-year Averaged δT_s for the Two Land Cover Conversions[a]

δT_s, °C	From OF to PP	From OF to HW
δT_s from longwave	−1.2	−0.9
δT_s from equation (5)	−1.8	−1.4
I. Eco-physiological/aerodynamic	−2.9	−2.1
II. Surface albedo	0.9	0.7
III. Ground heat flux	0.3	0.20
IV. Emissivity	−0.2	−0.1

[a]OF to PP and OF to HW. The contributions from the 4 components in the model (equation (5)) on δT_s are presented. OF is the abandoned old field ecosystem, PP is the pine plantation, and HW is the mature oak-hickory hardwood forest.

[19] As for albedo (term II), it is the major warming factor for both land-use conversion. We found that the warming effects due to albedo reductions alone following a conversion from OF to PP or OF to HW is much stronger in winter when compared to summer because albedo in OF is much higher than the two forests. The changes in albedo alone can warm the surface annually by 0.9°C for an OF to PP conversion, and by 0.7°C for an OF to HW conversion. As for the eco-physiological/aerodynamics component (term I), it is the major cooling factor for both land-conversions. The long-term cooling effects, estimated from Figure 4, are −2.9°C for the OF-to-PP conversion and −2.1°C for the OF-to-HW conversion (see Table 1).

[20] In conclusion, converting OF to PP or HW results in a surface cooling effect on annual time scales. Furthermore, unlike the boreal ecosystem study by *Betts* [2000], this cooling pattern is accompanied by increased CO_2 sequestration as evidenced by the EC based net ecosystem CO_2 exchange comparisons reported by *Stoy et al.* [2006b].

[21] **Acknowledgments.** This research was supported, in part, by the National Science Foundation (NSF-EAR 06-35787 and NSF-EAR-06-28432), the United States-Israel Binational Agricultural Research and Development (BARD, Research Grant No. IS3861-06), and the US Department of Energy (DOE) through the office of Biological and Environmental Research (BER) Terrestrial Carbon Processes (TCP) program (Grants # 10509-0152, DE-FG02-00ER53015, and DE-FG02-95ER62083).

References

Baldocchi, D. D., et al. (2001), FLUXNET: A new tool to study the temporal and spatial variability of ecosystem-scale carbon dioxide, water vapor and energy flux densities, *Bull. Am. Meteorol. Soc.*, *82*, 2415–2435.

Betts, R. A. (2000), Offset of the potential carbon sink from boreal forestation by decreases in surface albedo, *Nature*, *408*, 187–190.

Campbell, G. S., and J. M. Norman (1998), in *An Introduction to Environmental Biophysics*, Springer, New York.

Cess, R. D. (1978), Biosphere-albedo feedback and climate modeling, *J. Atmos. Sci.*, *35*(9), 1765–1768.

Charlson, R. J., F. P. J. Valero, and J. H. Seinfeld (2005), In search of balance, *Science*, *308*, 806–807.

Charney, J., W. J. Quirk, S.-H. Chow, and J. Kornfield (1977), A comparative study of the effects of albedo change on drought in semi-arid regions, *J. Atmos. Sci.*, *34*, 1366–1385.

Chen, Y., and S. Sun-Mack (2002), Surface Spectral Emissivity Derived from MODIS Data, paper presented at SPIE 3rd International Asia-Pacific Environmental Remote Sensing Symposium 2002: Remote Sensing of the Atmosphere, Ocean, Environment, and Space, Hangzhou, China, 23–27 Oct.

Feddema, J. J., K. W. Oleson, G. B. Bonan, L. O. Mearns, L. E. Buja, G. A. Meehl, and W. M. Washington (2005), The importance of land-cover change in simulating future climates, *Science*, *310*, 1674–1678.

Johnston, D. W., and E. P. Odum (1956), Breeding bird populations in relation to plant succession on the Piedmont of Georgia, *Ecology*, *37*, 50–62.

Katul, G. G., R. Oren, D. S. Ellsworth, C. I. Hsieh, N. Phillips, and K. Lewin (1997), A Lagrangian dispersion model for predicting CO_2 sources, sinks, and fluxes in a uniform loblolly pine (*Pinus taeda L.*) stand, *J. Geophys. Res.*, *102*, 9309–9321.

Novick, K. A., P. C. Stoy, G. G. Katul, D. Ellsworth, M. B. S. Siqueira, J.-Y. Juang, and R. Oren (2004), Carbon dioxide and water vapor exchange in a warm temperate grassland, *Oecologia*, *138*, 259–274.

Oren, R., B. Ewers, P. Todd, N. Phillips, and G. G. Katul (1998), Water balance delineates the soil layer in which moisture affects canopy conductance, *Ecol. Appl.*, *8*, 990–1002.

Otterman, J. (1977), Anthropogenic impact on the albedo of the Earth, *Clim. Change*, *1*, 137–157.

Parlange, M. B., and G. G. Katul (1992), Estimation of the diurnal variation of potential evaporation from a wet bare soil surface, *J. Hydrol.*, *132*, 71–89.

Pataki, D. E., and R. Oren (2003), Species differences in stomatal control of water loss at the canopy scale in a mature bottomland deciduous forest, *Adv. Water Resour.*, *26*(12), 1267–1278.

Priestley, C. H. B., and R. J. Taylor (1972), On the assessment of surface heat flux and evaporation using large scale parameters, *Mon. Weather Rev.*, *100*, 81–92.

Siqueira, M., G. G. Kutal, and C.-T. Lai (2002), Quantifying net ecosystem exchange by multilevel ecophysiological and turbulent transport models, *Adv. Water Resour.*, *25*, 1357–1366.

Stoy, P., G. G. Katul, M. B. S. Siqueira, J.-Y. Juang, H. R. McCarthy, H.-S. Kim, C. Oishi, and R. Oren (2005), Variability in net ecosystem exchange from hourly to inter-annual time scales at adjacent pine and hardwood forests: A wavelet analysis, *Tree Physiol.*, *25*, 887–902.

Stoy, P., et al. (2006a), Separating the effects of climate and vegetation on evapotranspiration along a successional chronosequence in the southeastern U.S., *Global Change Biol.*, *12*, 2115–2135.

Stoy, P., G. G. Katul, M. B. S. Siqueira, J.-Y. Juang, K. A. Novick, J. M. Uebelherr, and R. Oren (2006b), An evaluation of models for partitioning eddy covariance-measured net ecosystem exchange into photosynthesis and respiration, Agricultural and Forest Meteorology, *Agric. Forest Meteorol.*, *141*(1), 2–18.

Stull, R. B. (1988), *An Introduction to Boundary Layer Meteorology*, 666 pp., Kluwer Acad., Dordrecht, Netherlands.

Wear, D. N., and J. G. Greis (Eds.) (2002), *Southern forest resource assessment. Gen. Tech. Rep. SRS-53*, 635 pp., U.S. Dep. of Agric., For. Serv., South. Res. Stn., Asheville, N. C.

J.-Y. Juang, Department of Geography, National Taiwan University, No. 1, Sec. 4, Roosevelt Road, Taipei 10617, Taiwan. (jjuang@ntu.edu.tw)

G. Katul, K. Novick, and M. Siqueira, Nicholas School of the Environment and Earth Sciences, Box 90328, Duke University, Durham, NC 27708-0328, USA.

P. Stoy, School of GeoSciences, University of Edinburgh, 218 Crew Building, Edinburgh EH9 3JN, UK.